J. Fluid Mech. (1992), *vol.* 240, *pp.* 469–501
Printed in Great Britain

Direct evaluation of aeroacoustic theory in a jet

By JAMES BRIDGES† AND FAZLE HUSSAIN
Department of Mechanical Engineering, University of Houston, Houston, TX 77204-4792, USA

(Received 5 March 1991 and in revised form 19 December 1991)

This paper provides a unique, detailed evaluation of basic aeroacoustic theory applied to low-Mach-number ($M = 0.08$) cold jets. In contrast to most prior studies comparing theoretical predictions of jet noise with experimental results, our comparison uses a relatively complete knowledge of the flow field and employs vortex sound theory – an acoustic analogy which is shown to be insensitive to those aspects of the flow field about which our knowledge is incomplete. The primary result is that the measured sound field directivity of vortex ring pairing in circular jets is very similar to that predicted by theory: a stationary, axisymmetric, lateral quadrupole. This directivity is very unlike the monotonic polar dependence found in time-average measures of jet noise fields and unlike the directivity found in similar excited jet experiments. Although not perfect, the agreement between experiment and theory here is satisfyingly close in comparison to the discrepancies found by Huerre & Crighton (1983). Our result also proves that pairing of purely axisymmetric coherent structures is not the dominant sound source in low-Mach-number jets and that vortex asymmetry must be an essential aspect of the vortex motions which produce noise in such jets.

1. Introduction

Modern aeroacoustic theory has been around for approximately 40 years now, predominantly in the form of acoustic analogy theory where the equations of fluid motion are configured as the usual acoustic wave operator with remaining terms acting as an analogous source. Much effort has been devoted to transforming this source term – which includes nonlinear hydrodynamic terms and other terms involving viscosity, heat, etc. – into a form which is of finite extent and integrable. By far the most popular form is the one originally proposed by Lighthill (1952) which has successfully predicted global features such as scaling of total intensity with Mach number (M), jet diameter, etc., and to some extent, sound spectra and directivity. However, there has not yet been an exact, detailed validation of aeroacoustic theory applied to flows with extensive vorticity fields such as jet flows. This point was well stated by Huerre & Crighton (1983; hereinafter HC) who noted that almost all comparison between experiment and theory are made to test scaling laws which are relatively insensitive to flow details, and hence rather qualitative in nature. The reason for the lack of an exact comparison is obvious: one's knowledge of a turbulent jet flow is, at present, approximate, while most acoustic analogies are extremely sensitive to small errors in the description of the flow. Earlier attempts at 'proving' aeroacoustic theory in jet flows have required that both the precepts of the theory and a time-average turbulence model be tested simultaneously – no direct test of the

† Present address: Sverdrup Technology, Inc., NASA Lewis Group, 2001 Aerospace Parkway, Brook Park, OH 44142, USA.

theory being thus possible. While many hold that the existing evidence is strong enough, it remains a fundamental problem to show, by careful experiment and analysis, the degree to which the theory holds and why it fails.

The warnings against the validity of Lighthill's analogy are perhaps exemplified by the work of Crow (1970) and Lush (1971). Crow started by showing that the integrals which must be solved in Lighthill's analogy will not always converge – a problem shared by many analogies – unless the velocity field used is the solenoidal (incompressible) component of the total velocity field which decays fast enough away from the flow to guarantee convergence. Crow went on to recast the analogy as a coupled singular perturbation problem with small perturbation parameter M, asymptotically matching expansions in the near and far fields. By this process, he noted that the validity of the solution as an asymptotic series may end (as a result of the higher-order terms becoming larger than the lower-order terms) if the extent of the *rotational, incompressible* flow domain which constitutes the sound sources was more than an acoustic wavelength from the *irrotational, compressible* acoustic medium.

A similar conclusion was reached by Lush (1971) from his experiments designed to validate Lighthill's result in a jet. He also found that Lighthill's analogy did not predict well the far-field sound if the sound had travelled more than a wavelength through the jet. Because the wavelength of sound is inversely proportional to the jet speed, this factor becomes most crucial at higher M, just as Crow predicted.

The work of Lush was handicapped somewhat by the statistical nature of his knowledge about the velocity field and hence the presumed-known source (which he assumed to have uniform directivity). The work of HC proposed to rectify this by considering the sound produced by the orderly amplification and decay of excited instability waves in the shear layer of a jet. The decay of the instability wave is due to the growth of its subharmonic, the instability wave version of vortex pairing. They applied Lighthill's analogy to an instability wave model (based on experimental data of Laufer & Yen 1983; hereinafter LY) and calculated the far-field sound directivity for comparison with that measured by LY. The calculated sound directivity, though different from the experimental data, was of the same form until HC considered the axisymmetry of the problem and the cancellation of the sound produced around the jet. Because the wavelengths of interest in the problem were comparable to the diameter of the jet, even the form of the solution became significantly different as this cancellation produced an angle of extinction not present in the LY data. Figure 1 is a reproduction of figure 1 in HC showing the comparison between the LY data and the HC calculation. In their most recent work on the topic, Crighton & Huerre (1990) did not re-emphasize this critical point concerning the cancellation across the jet, thus leaving this glaring discrepancy unresolved.

In the present paper we are also trying to validate aeroacoustic theory applied to a jet, with some important differences from the work of HC. First, we are focussing our attention on motion at scales which allow the assumption that the entire jet diameter is acoustically compact. While HC found an angle of total destructive interference due to the non-compact source, the ratio of wavelength to jet diameter used here is more than 10 times greater than theirs. More importantly, we are using vortex sound theory, an acoustic analogy of the matched asymptotics variety, whose prediction of directivity, once the assumption of compact source is made, is insensitive to the errors in our approximations of the flow field (unlike the theory of Crighton & Huerre 1990). Our comparison, like that of HC, is in sound field directivity as the scaling laws from this theory are identical to that of Lighthill which

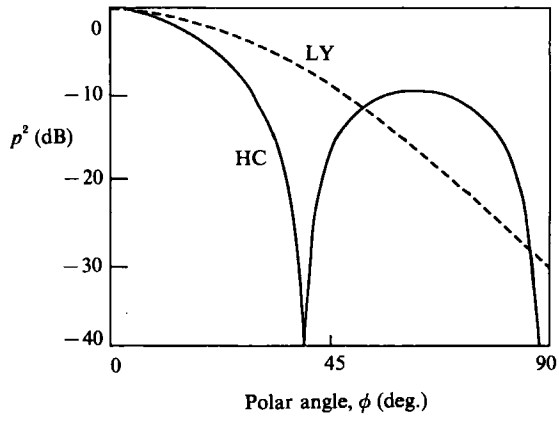

FIGURE 1. Reproduction of figure 1 of Huerre & Crighton (1983), comparing their theoretical directivity of sound from shear layer pairing and the directivity measured by Laufer & Yen (1983).

have been addressed in numerous previous studies. What makes this study unique is that both experiment and theory give directivities which have an unmistakable angle of extinction similar to that predicted by HC – a result clearly different from all reported jet directivity data. However, unlike HC, our extinction angle is a fundamental feature of the acoustic analogy solution, rather than a consequence of non-compactness. Our aim is to see if the exact asymptotic ($M \to 0$) solution given by acoustic analogy theory for the sound field of a jet bears any resemblance to the sound field of a real-world, small-Mach-number jet.

1.1. *Direct application of aeroacoustic theory*

Kambe (1986) has shown that vortex sound theory (Möhring 1978; Obermeier 1985), and by extension all acoustic analogy theory (Howe 1975), is valid for simple flows which very nearly meet the very strict assumptions of such theory. These flows (well-defined vortex ring collision, vortex/surface interaction), aside from having tractable flow fields, have been carefully chosen to remove the three greatest difficulties faced when applying the theory to turbulent free shear flows – non-compact sources, source advection and extensive vorticity fields.

The accuracy of the prediction of sound by any acoustic analogy theory appears to rest first on the degree to which the application meets the assumptions made in deriving the theory and second on the sensitivity of the theory to the unavoidable errors made in specifying the flow field. Before one can determine the error due to not meeting the assumptions of the theory, one must address this second problem. The flow field of a jet is, in general, too complex and too detailed to be characterized in such a way as to satisfy the requirements of the theory. By careful construction we have created a facility which can produce a highly organized jet flow at a high enough (though still small) Mach number to produce measurable sound in an anechoic environment. We then proceed to measure the flow and sound fields, calculating the time-dependent vorticity field from the conditionally (phase) averaged velocity data. We choose to use the vorticity form of acoustic analogy theory because of its linearity in the flow field variable, which allows us to relate conditionally averaged vorticity to conditionally averaged sound. Having overcome the problem of accurately specifying the flow field, all that is left to cause disagreement between theoretical and experimental results is the satisfaction of assumptions – that, and the

inaccuracy of the theory! Therefore, we now briefly discuss the assumptions made in the application of vortex sound theory to jets.

Compact-source assumption

Because vortex sound theory uses Mach number M as a small perturbation parameter, the fundamental assumption of the theory is that $M \to 0$. In the sound generation process, the timescales of motion and of sound must be equivalent; therefore, the assumption of small M is synonymous with the assumption of a compact source. By compact source, one means that the lengthscale of the flow l, i.e. the region of flow which can be considered as an independent source, is much smaller than the wavelength λ of sound being produced. When the flow is viewed as a collection of spatial structures which are independent sound sources, the compact-source assumption becomes the assumption that the structures cover a distance $(l+M\lambda)$ which is small compared to λ during the time they emit the sound. In the light of recent understanding of coherence structures in jet, one might consider the jet diameter to be the relevant flow lengthscale in the potential core of the jet, with the axial lengthscale being determined by the lifetimes of the coherent structures and their advection speed. In the limit of $M \to 0$, of course, the advection speed vanishes, eliminating the 'stretching' effect of advection. As with any asymptotic theory, however, one does not know how well the asymptotic solution can be applied to situations away from the asymptotic limit.

An interesting situation arises when the flow structures themselves are advecting but their motion is such that they produce sound only at a fixed point, thus creating a *stationary source*. The colliding vortex rings studied by Kambe (1986) are an example of such a flow, as is the case of spatially fixed, periodic pairing of vortex rings in a jet. Because the formation and subsequent interactions (leapfrogging, pairing) of several consecutive vortex rings are often correlated, l is larger than the vortex ring size, encompassing multiple ring pairs. To study the vortex pairing interaction as a single source, only frequencies corresponding to λ much larger than l should be considered.

Compact-flow assumption

Most acoustic analogy theory assumes that the sound, once generated, has no effect on the vorticity of the flow through which it propagates and that the vorticity has no effect on the propagating sound. This apparently innocuous assumption, which Crow (1970) dubbed the *compact flow* assumption, is critical, as was discussed in the introduction. Sound travelling through a vortical field for more than a wavelength is modified by its interaction with vorticity (scattering) and also modifies the vorticity field, either effect requiring additional terms of the same order in M in the sound source expression if the far-field result is to be correct. Because of Crow's analysis showing that these additional terms may come to dominate the first-order (Lighthill) term, there is reason to doubt whether an appropriate acoustic analogy can be formulated for jet flows, particularly in predicting the sound emitted at angles (near the jet axis) where the sound must travel several wavelengths through the vortical flow to reach the acoustic ambient.

It should be noted that the sound scattering effect is subsequent to the sound generation and so does not significantly change the total sound intensity emitted, as measured by integrating over a sphere around the jet exit. The effect of the vorticity being modified by the sound wave on the total sound intensity is unknown, but may not be large except in special cases (e.g. Broadbent & Moore 1979). Therefore, it is

quite possible that these effects will only appear in predictions of the sound directivity and not in scaling laws which have been the main measures by which the theory has been judged.

Free-space and inviscid flow assumptions

Though not a fundamental assumption of aeroacoustic theory, surface terms are usually neglected when applying the theory to jet noise (Curle 1955); in particular, these terms were neglected by HC. When calculating the sound produced by jet flows, the surface terms representing flow/surface interaction and the acoustic effects of reflection and diffraction by the nozzle body should be included. Consideration of the effects of the nozzle will be covered in a future paper; here we ignore interaction of solid body and flow except in the discussions. Likewise, most applications of aeroacoustic theory to high-Reynolds-number flows ignore the sound produced by purely viscous effects. We will also make this assumption, supported by the arguments of Obermeier (1985).

1.2. *Overview of this study*

Our approach to verifying that aeroacoustic theory can be applied to jet consists of a series of steps involving detailed measurements, simple analysis and direct comparison. The first step (§2) is to briefly review vortex sound theory and a few of its basic features: in particular, the fundamental prediction that the sound produced by a compact axisymmetric distribution of vorticity is uniquely described by an axisymmetric lateral quadrupole (hereinafter abbreviated as *axiquad*). The second step is to make measurements in an excited jet where the flow field can be known with considerable accuracy. Both standard measurements (to verify that the results found are not the consequence of any jet rig anomaly) and conditionally averaged measurements of the vorticity and sound pressure fields are presented. It will be shown (§3) that the vorticity field is axisymmetric in keeping with the analysis of §2, and that the vorticity field measured is the one essentially producing the sound being measured (§4). The next step is to compare the sound pressure fields measured with those predicted by theory and seek explanations for any discrepancies (§5).

2. Vortex sound theory

2.1. *Brief review*

Powell (1964) first expressed the acoustic analogy problem in terms of vorticity, followed by Möhring (1978), Obermeier (1985) and Kambe (1984), who gave the theory rigorous treatment by application of matched asymptotic expansions and singular perturbation methods, transforming the expression for sound into a linear function of vorticity. This thus provides a 'linear theory' for an intrinsically nonlinear situation. The latter two authors have extended the theory to viscous flows, both showing that viscous motions in a cold flow contribute a sound field component $p_{\mathrm{vis}}(\boldsymbol{x}, t)$ which is monopole in nature and relatively weak:

$$p_{\mathrm{vis}}(\boldsymbol{x}, t) = \frac{(5-3\gamma)\,\rho_0}{12\pi c_0^2 |\boldsymbol{x}|} \frac{\partial^2}{\partial t^2} K, \tag{1}$$

where K is the kinetic energy of the flow, γ is the ratio of specific heats, c_0 is the speed of sound, and ρ_0 is the mean fluid density. Kambe (1986) presents a general solution for vortex-induced sound in the presence of a solid surface $\mathscr{S}$ by matching a

multipole expansion of the far-field pressure p_{F} (outer solution) with a near-field pressure p_{I} (inner solution) of the form

$$p_{\mathrm{I}} = -\rho_0 \int \boldsymbol{N}(\boldsymbol{y},t)\cdot\boldsymbol{\nabla}\boldsymbol{y}\, G\, \mathrm{d}^3 y, \tag{2}$$

where G is a Green's function and $\boldsymbol{N} = (\boldsymbol{u}\cdot\boldsymbol{\nabla})\boldsymbol{u}$, satisfying

$$\boldsymbol{\nabla}\cdot\boldsymbol{u} = 0, \quad \boldsymbol{n}\cdot\boldsymbol{u} = 0,$$

for the unit normal $\boldsymbol{n}$ on the boundary of $\mathscr{S}$, and

$$\boldsymbol{n}\cdot\boldsymbol{\nabla}\boldsymbol{y}\, G = 0 \quad \text{for} \quad \boldsymbol{y} \text{ on } \mathscr{S}.$$

After accomplishing the matching for the specific cases where there exists (i) no solid body, (ii) a compact solid body, and (iii) a non-compact solid body, far-field solutions are obtained which recover the results of (i) Möhring (1978) (axiquad), (ii) Curle (1955) and (iii) Ffowcs Williams & Hall (1970) (cardioid pattern), respectively.

Although the formal solution (2) is complicated, the interpretations made in each of the first two cases (i) and (ii) are invaluable for predicting the sound produced by flows with vorticity concentrated in vortex tubes forming closed loops, such as vortex rings. The interpretation is as follows. To find the sound intensity at a far-field point, construct a fictitious potential flow with *vector stream function* $\boldsymbol{\Psi}$ around the solid body which, in the far field, is parallel to the direction of observation and of unit magnitude. In the case of free-space flows, this is a uniform vector field. Near a solid body, as the vortex ring traverses this fictitious flow the volume flux through the ring will in general be an unsteady function of time. The sound pressure at the far-field point of observation is then given by time derivatives of the moments of this flux,

$$\left.\begin{aligned} p_{\mathrm{F}}(\boldsymbol{x},t) &= \frac{\rho_0}{c_0}\frac{x_i}{x^2}\frac{\partial^2}{\partial t^2}\Pi_i\left(t-\frac{x}{c_0}\right), \\ \Pi_i(t) &= \frac{\Gamma}{4\pi}\int_S (\boldsymbol{\nabla}\times\boldsymbol{\Psi}_i)\cdot\boldsymbol{n}\,\mathrm{d}S, \end{aligned}\right\} \tag{3}$$

where S is the surface having a vortex ring as its perimeter, Γ is the circulation of this vortex ring, and $\dot{\Pi}_i$ is the dipole coefficient.

In the case of vortex motion near solid bodies, the dipole component is non-zero. The changes in the fictitious potential flow near the body give rise to changes in its volume flux through vortex rings even if they are steadily advecting; their passage near a surface will, therefore, produce a dipole source. In free space, the fictitious potential flow is uniform, and thus a steadily translating vortex ring has a steady volume flux. This will make Π_i = constant, leaving only quadrupole and higher-order multipole terms. The quadrupole terms can be shown to be equivalent to those of Möhring (1978; as commonly expressed, e.g. Bridges & Hussain 1987):

$$p(\boldsymbol{x},t) = \frac{\rho_0}{x^3 c_0^2}\frac{\partial^3}{\partial t^3} x_i x_j Q_{ij}\left(t-\frac{x}{c}\right), \tag{4}$$

$$Q_{ij}(t) = \frac{-1}{12\pi}\int_V y_i (\boldsymbol{y}\times\boldsymbol{\omega})_j \, d^3 y. \tag{5}$$

The constraints on the quadrupole source tensor are

$$Q_{ii} = 0, \tag{6}$$

$$\frac{\partial}{\partial t} Q_{ij} = \frac{\partial}{\partial t} Q_{ji}. \tag{7}$$

The former of these is a simple consequence of the fact that $\boldsymbol{y}$ is orthogonal to $\boldsymbol{y}\times\boldsymbol{\omega}$; therefore, by definition of the dot product, $y_i(\boldsymbol{y}\times\boldsymbol{\omega})_i$, and hence Q_{ii}, must be zero. The symmetry of $(\partial/\partial t)Q$ can be shown by noting that the moment of impulse

$$\boldsymbol{M}=\frac{\rho}{3}\int \boldsymbol{y}\times(\boldsymbol{y}\times\boldsymbol{\omega})\,\mathrm{d}^3y$$

is a conserved quantity in incompressible inviscid flows, and that $\epsilon_{ijk}Q_{ij}\sim M_k$ (e.g. $(\dot{Q}_{12}-\dot{Q}_{21})\sim\dot{M}_3\equiv 0$).

2.2. *Principal result for axisymmetric vorticity in free space*

In axisymmetric flows with no source advection, the integral constraints (6) and (7) dictate the sound field directivity exactly. Axisymmetry requires that

$$Q_{22}=Q_{33},$$

where x_1 is the ring axis, and by (6),

$$Q_{11}=-2Q_{22}=-2Q_{33}.$$

Further, $Q_{ij}=0$ for $i\neq j$, because $y_i(\boldsymbol{y}\times\boldsymbol{\omega})_j$ is odd across the ith axis, making its integral vanish. Taking into account the direction cosines in (4), we find that the directivity is identically that of an axiquad with polar angles of extinction $\phi^*=54.7°$ and $\phi^{**}=125.3°$. *This is the directivity of all sound produced by compact, inviscid, axisymmetric vortical motion in the absence of solid surfaces.* While the temporal behaviour of the coefficients Q_{ij} will depend greatly upon the evolution of the axisymmetric vorticity field and hence upon the uncertainty in our knowledge of the vorticity field, the constraints on $\dot{Q}_{ij}$ dictate that the *directivity* will remain the same. This is important because it shows that the theory's prediction of directivity is sensitive only to the axisymmetry of the flow and not to other aspects of the approximation of the vorticity field.

2.3. *Theoretical prediction of sound from axisymmetric jets*

It is easily shown that the axisymmetric vortical motions commonly called 'pairing' cause strong fluctuations in the coefficients $\ddot{Q}_{ij}$ (Kambe & Minota 1981). If the jet flow is viewed as an axisymmetric vorticity field in free space which undergoes such pairing, the theory predicts that such a flow will produce an axiquad sound field which has a directivity very unlike jet noise as it is reported in the literature (e.g. Lush 1971; Ahuja 1973; Moore 1977). Therefore, if vortex sound theory is found to apply to jets which approximately meet the assumptions stated above, axisymmetric vortex pairing is not a dominant sound source in such jets. This does not rule out non-axisymmetric motions which involve merger of three-dimensional vortices, such as those considered by Möhring (1990). The dissertation of Bridges (1990) discusses the effect of three-dimensional motions as predicted by theory, which produces directivities closer to that of jet noise. Given the fundamental result of §2.2, and the fact that jet noise directivity reported in the literature shows not the least indication of an extinction angle, it follows that axisymmetric vortex pairing cannot be the dominant sound source in jets – provided, of course, that the theory is proven applicable to jets, as it will be. Even considering the smearing of the directivity by jitter in pairing location and time (a simple exercise in superposition of quadrupole sources) the extinction angle would still be clearly evident at the frequencies which contain most of the jet noise energy, i.e. $St_D<1$, in low-Mach-number jets, the compactness of these sources, $\lambda/D=(St_D M)^{-1}$ being sufficient to meet the assumptions of the theory.

2.4. *Principal result when surface terms are not zero*

When solid surfaces are present, an additional dipole term must be added to the quadrupole. If the surface and vorticity are axisymmetric and coaxial, the addition of the dipole will shift the extinction angles, i.e. the polar angles at which no sound is radiated; the exact shift will depend on the relative strengths and phases of the two sources. In addition, the dipole and quadrupole will not necessarily have similar temporal behaviour because $\Pi_i(t)$ and $\Theta_{ij}(t)$ are different functions of the vortex motion.

2.5. *Why use vortex sound theory?*

Why is the free-space vortex sound theory special to this study? Put simply, this is because

$$p(\langle\omega\rangle^*) = \langle p(\omega^*)\rangle; \tag{8}$$

that is, conditional averages (or phase averages; denoted by $\langle p\rangle$) of the sound pressure are predicted exclusively from conditional averages of the vorticity with proper consideration of retarded time (*) for regions greater than a fraction of a wavelength. This is not true for other versions of aeroacoustic theory in which the sound pressure is a nonlinear function of velocity:

$$\langle p(u_i u_j)\rangle = p(\langle u_i\rangle\langle u_j\rangle) + p(\langle u_i' u_j'\rangle).$$

Thus, conditional averages of the sound field involve not only the conditional averages of the velocity field but also the correlation of the remainder terms, u_i'.

If the same averaging criteria are applied to both vorticity and sound fields, (8) states that the sound calculated using conditional averages of the vorticity field and of the measured conditional-average sound field should be the same. As an aside, this is also the basis for a precise understanding of the sound produced by coherent structures which are educed by conditional, phase-aligned ensemble averaging.

3. Experimental facilities

Studies such as this require utmost care not only in facility design and validation, but also in documentation of the flow's condition at the jet exit. We feel that our study is distinguished by our careful work in these areas. Full documentation, while clearly important, requires lengthy discussion and would constitute a major digression if placed at this juncture; hence the full description of the facility and of our baseline data has been consigned to Appendix A while the main parameters of the jet facility are given in table 1. The initial condition definitely qualified as 'nominally laminar' in the terminology of Hussain (1983). The low free-stream and boundary-layer turbulence intensity levels achieved here undoubtedly made possible the high degree of control which was necessary for successful application of the simple conditional averaging of the flow and sound fields.

The results presented later are so striking compared to data usually found in jet noise papers that we feel compelled to produce data showing the unexcited jet for comparison with other jet rigs, indicating that the results presented later are not the product of any artifact in our facility. Figure 2 presents standard overall sound pressure level (OASPL) measurements made in the unexcited jet for the range of polar angles studied. The Mach number of the jet for these measurements was slightly higher ($M = 0.15$) than it was for the excited jet ($M = 0.08$) because the unexcited jet at $M = 0.08$ did not produce sound levels sufficiently above the ambient to measure accurately. Data were repeatedly acquired and processed in blocks until the variance between estimates of r.m.s. for each block was less than 1%; this typically involved

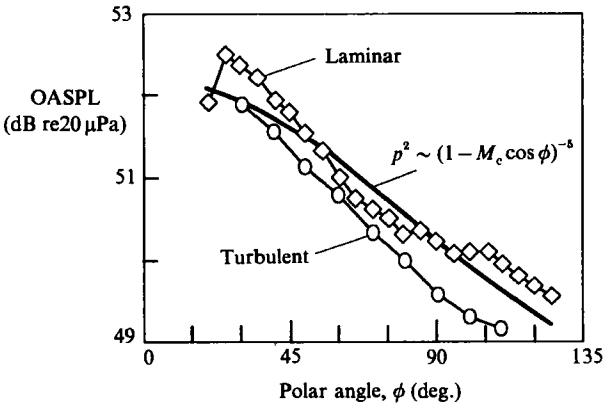

FIGURE 2. OASPL directivity of the jet with laminar and turbulent initial condition at $M = 0.15$ compared with the conventional result of Lighthill (1952). The theoretical curve is adjusted to match experiment (laminar condition) at $\phi = 90°$.

Jet diameter		D	4 cm	
Jet speed (unless indicated otherwise)		U_j	27.7 m/s	
Free-stream turbulence intensity on jet centerline		u'/U_j	0.0004	
Maximum boundary-layer turbulence intensity		$u'(y = \delta^*)/U_j$	0.001	
Momentum thickness		θ_e	0.141 mm	
Shear-layer instability frequency		f_{sl}	2575 Hz	
and Strouhal number		St_{θ_e}	0.0131	
Excitation frequencies and amplitudes used	f_{ex}	f_c	St_D	u'_f/U_j
Stable pairing (SP) flow	606 Hz	303 Hz	0.87	0.008
Stable double pairing (SDP) flow	770 Hz	193 Hz	1.14	0.007

TABLE 1. Parameters of flow facility and statistics of initial condition. δ^* is the nozzle exit boundary-layer displacement thickness, typically the location of peak turbulence intensity; f_{ex} is the excitation frequency and $1/f_c$ is the period of the conditional average. $St_D = f_{ex}D/U_j$. u'_f is the longitudinal r.m.s. velocity in the excited jet measured at the jet exit.

averaging over 30–60 s of data. The directivity was quite repeatable to within a fraction of 1 dB even though the absolute level of the sound was only repeatable to within 1 or 2 dB, presumably due to difficulties in resetting the blower controller from day to day. The sound level given is that after the subtraction of approximately 35 dB of background noise – a rather small correction. Three curves are shown in figure 2: two are data taken in the jet with laminar and turbulent initial conditions, the third is the conventional Lighthill directivity arising from the advection of uniform sources. The predominant sound source in the laminar initial condition was the pairing of shear-layer vortices at $St_\theta \approx 0.007$ (Bridges & Hussain 1987); this caused the slightly irregular directivity shown. When the nozzle boundary layer was tripped, the directivity became more like that of Lush and others.

4. Experimental results

4.1. *Conditions of the flow and sound fields*

Two excited flows are studied in this paper: 'stable pairing' flow (SP; Zaman & Hussain 1980) with a single fixed pairing and 'stable double pairing' (SDP) flow with two fixed vortex pairings; the excitation parameters are given in table 1. Figure 3

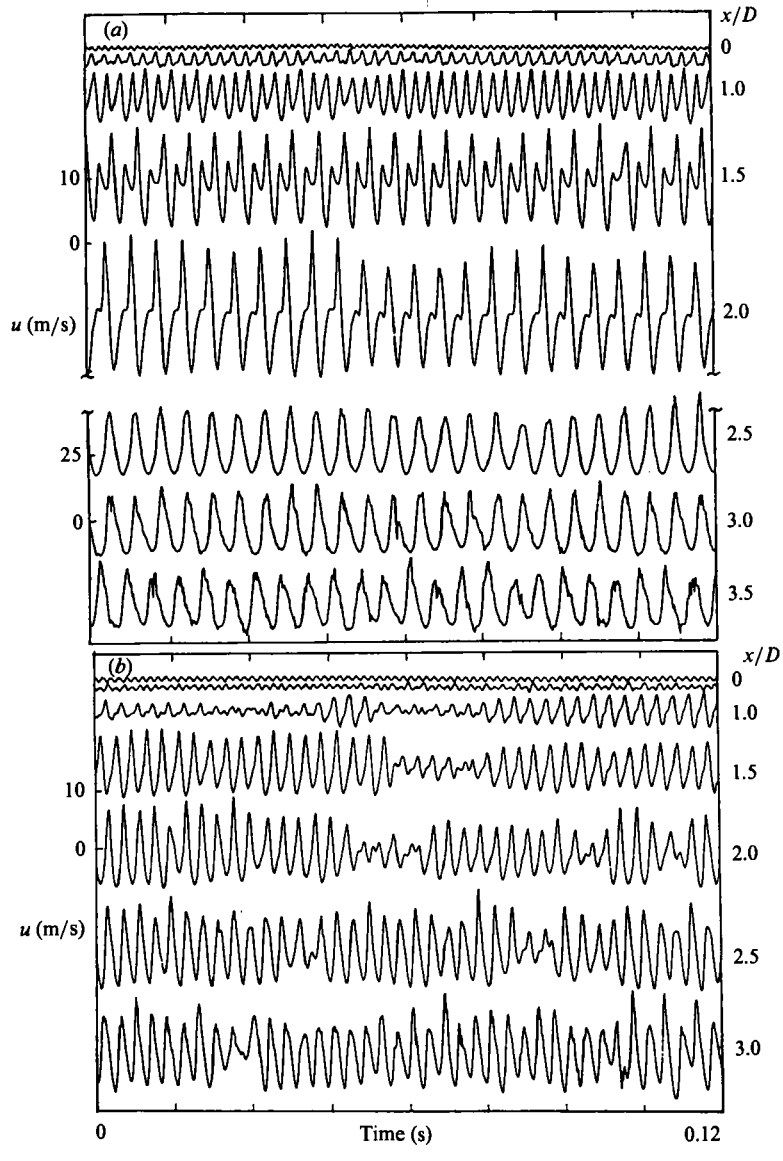

FIGURE 3. Centreline velocity signals at different axial locations. (*a*) $u_t'/U_j = 0.75\%$, $St_D = 1.14$ (SDP); (*b*) $u_t'/U_j = 0.95\%$, $St_D = 0.88$ (SP). Note the break in the ordinate scale in (*a*).

shows velocity signals taken at different axial locations indicating how 'stable' or periodic the SP and SDP flows were found to be. The SP flow was not as stable as the SDP flow, nor as steady as that studied in Zaman & Hussain (1980); the most likely reason is that the former study used an excitation level u_t'/U_j over 0.02 while the present study used only 0.008. The excitation amplitude was constrained by the total power available from the speakers and by the dynamic range of the analog-to-digital convertor which must discriminate the aeroacoustic sound from the excitation tone. The SDP flow was not only very stable, but had at least two pairing interactions, making the study of sound by pairing even more interesting. This flow was found for a limited range of excitation amplitudes and has since been duplicated in a smaller, totally independent, jet facility in a separate room. The flow was highly

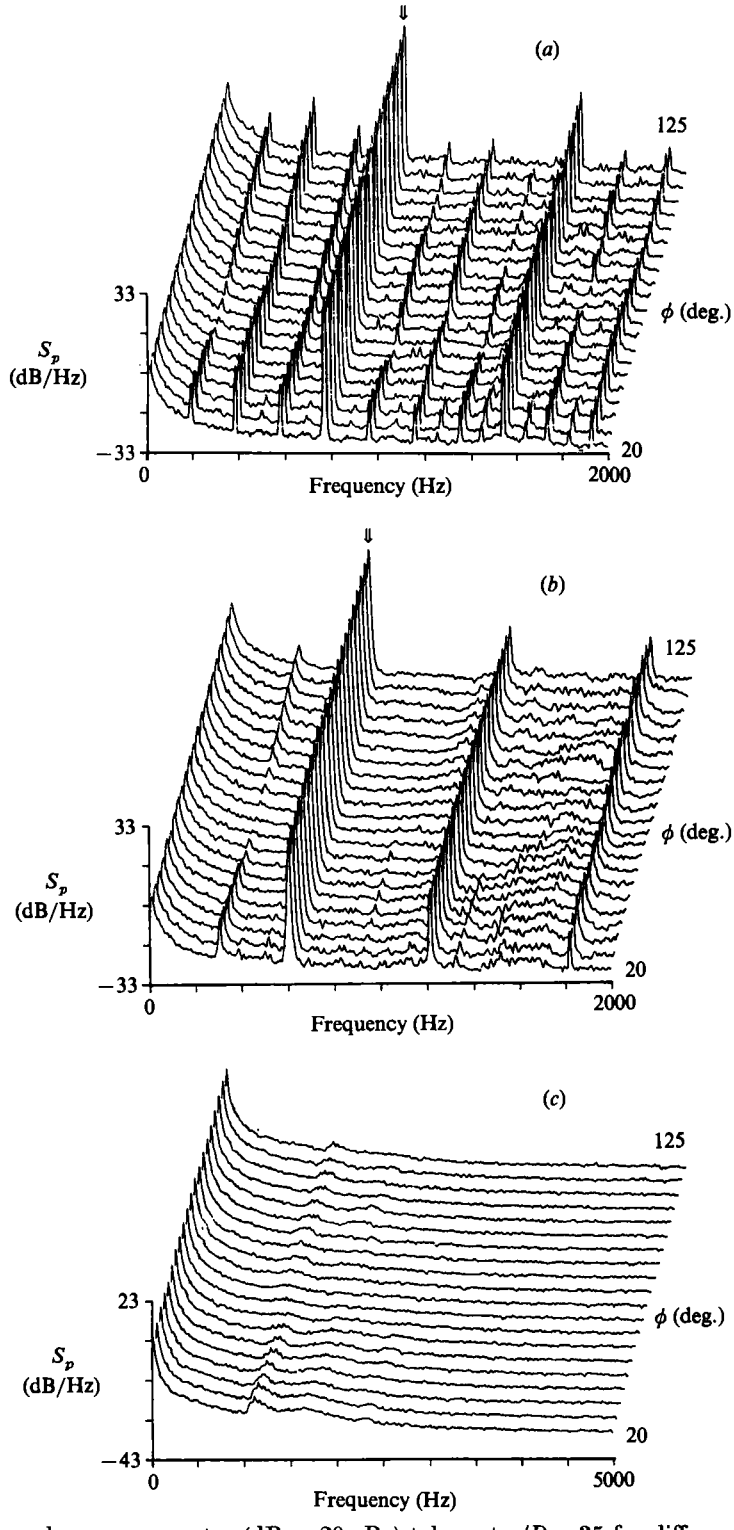

FIGURE 4. Sound pressure spectra (dB re 20 μPa) taken at $r/D = 35$ for different polar angles ϕ ($\Delta\phi = 5°$). (*a*) SDP flow, (*b*) SP flow, (*c*) unexcited flow. The arrow indicates the excitation frequency.

dependent on excitation amplitude, indicative of a tuned flow situation, possibly caused by feedback of the subharmonics and optimal subharmonic resonance.

Standard measures of the sound field also indicated an extremely periodic, highly tuned jet flow. Figure 4 gives the sound pressure spectra for the two flows as functions of polar angle taken at $r/D = 35$. The excitation tone, indicated by an arrow, causes the flow to produce clear subharmonic tones which have interesting spatial dependence. Although it is not easily seen in this presentation, the frequency of the subharmonic peaks are independent of polar angle, signifying that the acoustic sources are fixed, not advecting – an observation regarding the tones of pairing vortices made previously by others as well (LY; Bridges & Hussain 1987). Take note of the change in amplitude of the subharmonic peaks with polar angle: these essentially give the directivity of the sound produced by the pairing of vortices in the excited jet, although the effect is muted somewhat (especially $\frac{1}{2}f_{ex}$ in figure 4*a*) compared to the conditionally averaged data presented later. A similar directivity is noted in the odd harmonics of the second pairing frequencies (i.e. $\frac{3}{4}f_{ex}$, $\frac{5}{4}f_{ex}$, etc. in figure 4*a*), which are uncontaminated by harmonics of the excitation tone and of the first pairing frequency, $\frac{1}{2}f_{ex}$. This directivity again shows up in the unexcited jet spectrum (figure 4*c*, taken at $r/D = 35$) at the subharmonic of the natural instability frequency of the shear layer, presumably caused by the pairing of shear-layer vortices.

4.2. *Conditionally averaged measurements of the vorticity field*

As mentioned in the introduction, one of the biggest difficulties in comparing aeroacoustic theory with jet noise experiments is that the knowledge of the velocity field in most jets is very approximate. This was mitigated somewhat in this study since the jet was excited in the receptivity band of the jet column instability, making the jet vorticity field consist of periodic, axisymmetric vortex rings and producing a very robust phase average of the vorticity field. The subharmonic content of the signal was also strong, possibly due to feedback, producing spatially fixed vortex pairing which was the dominant sound source. The criteria for the conditional averages were that the fields (i) be axisymmetric and (ii) have subharmonic strengths and phases within a small deviation of their most probable values.

The axisymmetry of the velocity field, and by extension the vorticity field, was quantified by making azimuthal decompositions of the velocity field measured using four hot wires around the jet at different axial locations. Figure 5 gives the evolution of the first two azimuthal modes for the unexcited, SP and SDP flows over the measurement domain. Detailed analysis (Bridges 1990) found that modes ± 1 were of similar amplitude and often of the same phase, indicating that the asymmetry was better described as tilting of rings rather than as a helical vortex. Of course, it must be remembered that with only four azimuthal probes, modes 4, 8, 12, ... are aliased into mode 0 while modes 3, 5, 7, ... are aliased into mode ± 1. It is unlikely, however, that the higher modes are significant when the mode 0 component is much stronger than mode ± 1. Therefore, the signal from a single local sensor was used for the conditional sampling under the assumption that the SDP flow was axisymmetric for the entire domain and that the SP flow was axisymmetric for at least the first three diameters where the vortex pairing takes place.

The velocity record from the single long-prong hot wire (used to avoid shear-layer tone; Zaman & Hussain 1978), located at $x/D = 1.25$, $y/D = 0.25$, was used as a trigger signal and the velocity at the measurement location was accepted only if the trigger signal satisfied criteria based on the first few Fourier coefficients of the trigger signal. In this procedure, the trigger signal was broken into segments one fundamental

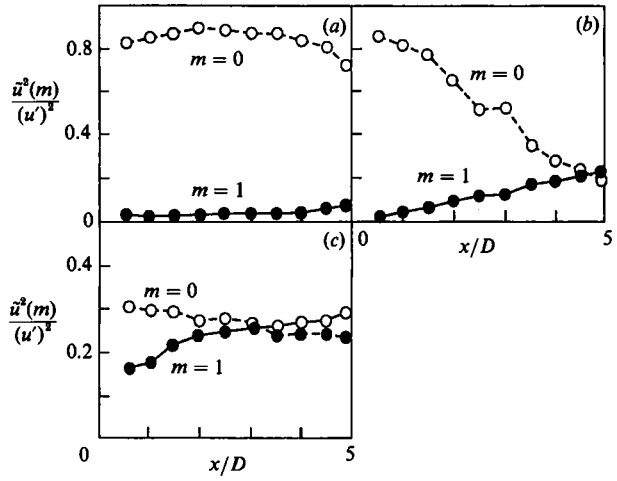

FIGURE 5. Magnitude squared of first two azimuthal modes as functions of axial distance for (*a*) SDP flow, (*b*) SP flow, (*c*) unexcited flow.

period long ($4/f_{ex}$ for the SDP flow, $2/f_{ex}$ for the SP flow) using the excitation signal. The first few Fourier coefficients of the signal were computed for each segment and a multi-dimensional probability density function was constructed with the axes being the real and imaginary Fourier coefficients. The probability space was checked for multiple modes, but found to consist of only one dominant mode.

Threshold values for conditional averaging were set around the peak in the multi-dimensional probability distribution such that 99% and 74% of all periods were accepted for the SDP and SP flows, respectively. During data acquisition, signals were acquired from both the fixed-location trigger sensor and an $\times$-wire traversed in an axial plane over the region $0 < x/D < 5$, $0 < y/D < 1.2$, with periods of the $\times$-wire signal being accepted only when the trigger signal passed through the window defined by the threshold values. As an additional precaution against including any exceptional structures which might fortuitously possess passable Fourier coefficients, each accepted trigger signal record was correlated with its ensemble and those which did not correlate well (within a threshold value) were rejected along with the corresponding $\times$-wire record. The ensemble average and correlation procedures were iterated until all segments passed a correlation threshold of 0.99 (SDP) or 0.9 (SP). (In the SDP flow 178185 of the 179367 sampled frames were accepted; 210892 of 286638 of the sampled frames were accepted in the SP flow.) The vorticity field was then obtained by spatial derivatives of a bicubic spline fitted to the velocity field which was measured on a non-uniform grid designed to resolve the high gradients near the jet and along the lip line.

Figure 6 shows the periodic conditional (phase) average of the vorticity field $\langle\omega\rangle$ as calculated from the *unsmoothed*, conditionally averaged velocity for the SDP and SP flows. The SDP flow is strongly two-dimensional, as evidenced by the strong conditionally averaged vortices. In the SP flow, three-dimensionality sets in quickly after $x/D = 3$ and the conditionally averaged vorticity is weakened significantly. From these data one can clearly see vortex pairing and fix the location where the vortices are coplanar, which will be defined as the 'location' of pairing; this is the instant when the sound waveform reaches a maximum amplitude according to theory (see Kambe & Minota 1981) and thus are the source locations, identifiable to within a fraction of a jet diameter. The vortex interactions of the SDP flow are very

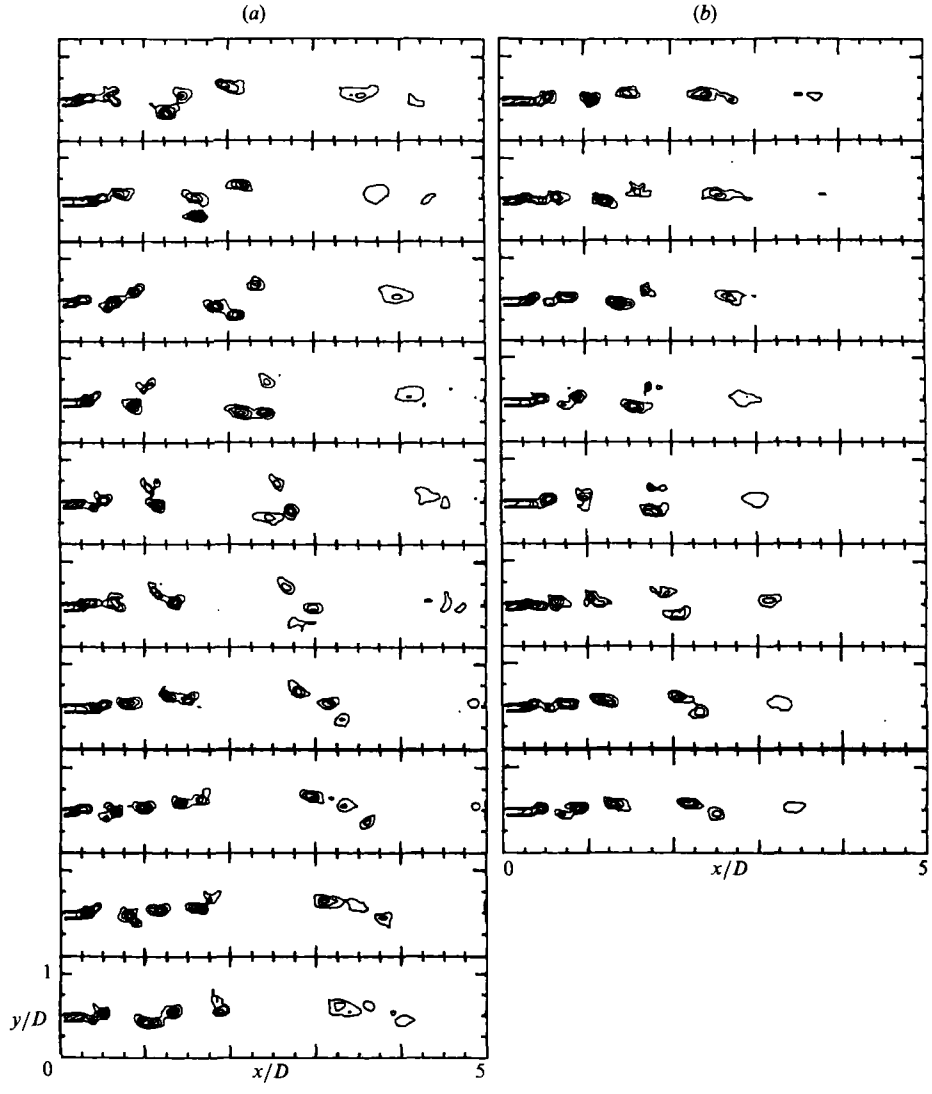

FIGURE 6. Conditionally averaged vorticity $\langle\omega\rangle/f_{ex}$. (a) SDP flow ($\Delta t = 0.512$ ms between panels), (b) SP flow ($\Delta t = 0.384$ ms). Contour interval = 2.0, lowest contour = 4.0.

complicated; nominally the interaction location for the $\frac{1}{4}f_{ex}$ pairing is at $x/D = 2.5$. However, a careful study of the data (only 10 of the 40 frames sampled in the period are shown here) shows that the vortex interactions are sometimes complete mergings and sometimes simple passthroughs without merger. Figure 7 presents maps of the vortex interactions, indicating the locations, phases and types of interactions which occur in the two flows. In each flow, the vortices formed at the excitation frequency are actually the result of merging of vortices which have been formed by the shear-layer instability, but are too small to be resolved by the $\times$-wire. The shear layer is unstable to perturbations in the range $St_\theta = f\theta/U_j = (0.011, 0.018)$; therefore, the first vortices which can be identified in the SDP flow (corresponding to $St_\theta = 0.004$) are presumably the product of two pairings of vortices initially formed at 0.016, as are the first vortices in the SP flow (corresponding to $St_\theta = 0.0031$, or 0.013/4). These initial shear-layer interactions produce sound at higher harmonics of the excitation

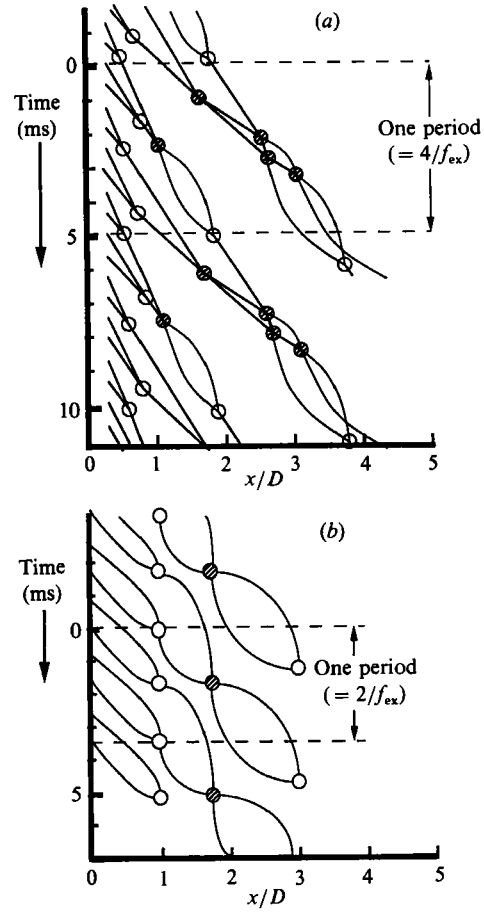

FIGURE 7. Vortex interaction schematic for (*a*) SDP flow and (*b*) SP flow. Open circles indicate complete mergers of vortices, hatched circles indicate leap-frog interactions.

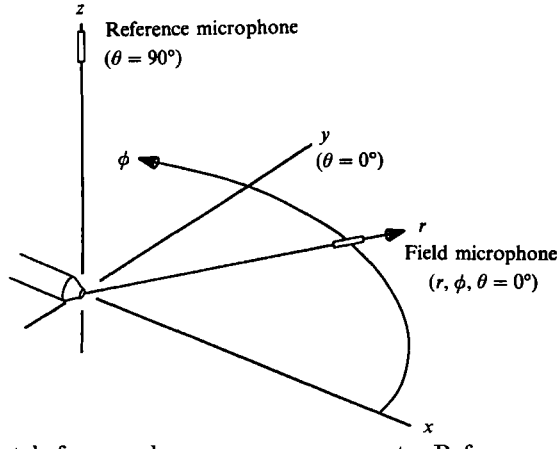

FIGURE 8. Orientation sketch for sound pressure measurements. Reference microphone located vertically above the jet exit at $r = 35D$, $\phi = 90°$, $\theta = 90°$. Sound pressure measured in $(r, \phi, \theta = 0°)$ plane.

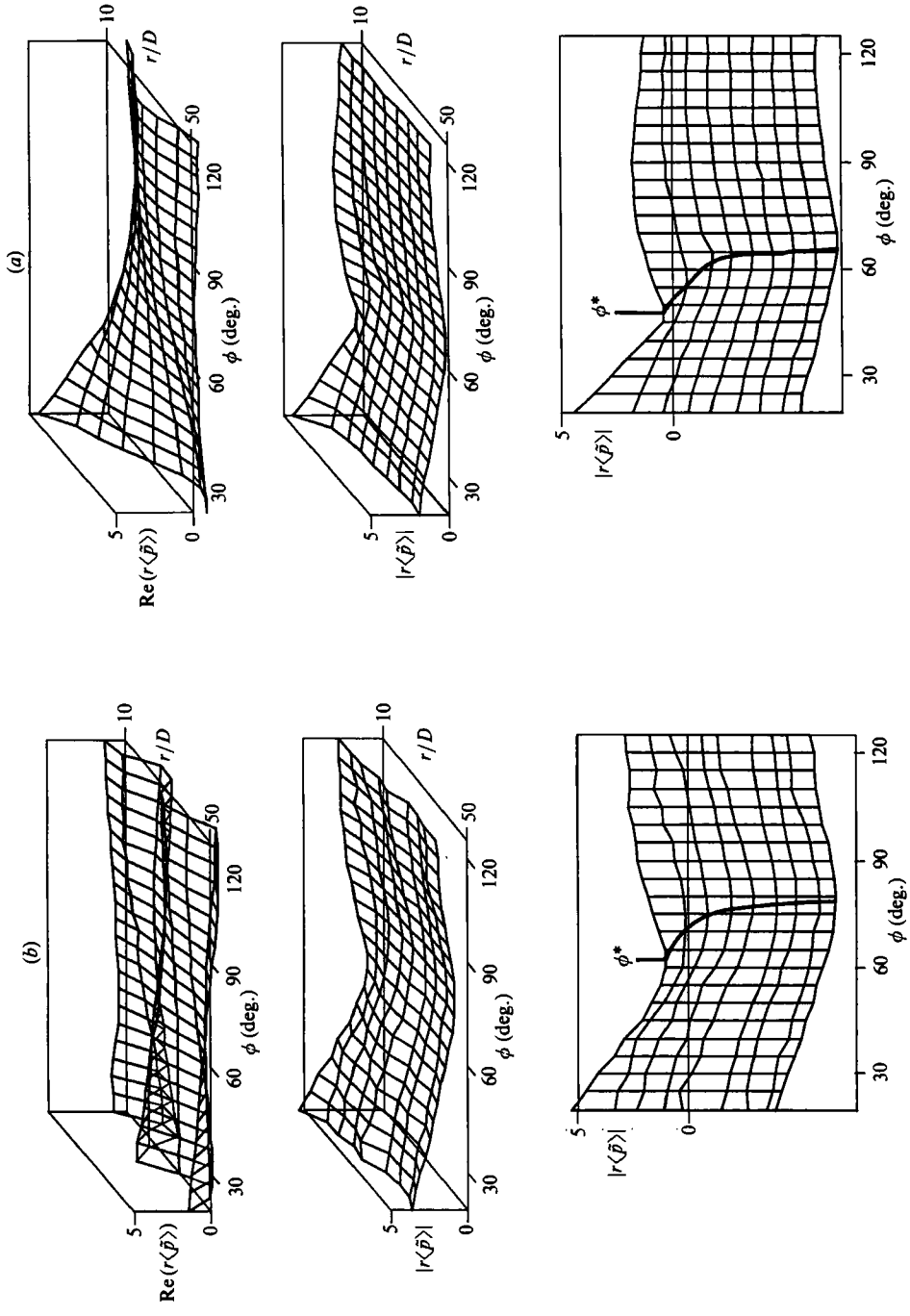
(a)
(b)
Re(r⟨p̃⟩)
|r⟨p̃⟩|
r/D
ϕ (deg.)
ϕ*
0
5
10
30
50
60
90
120

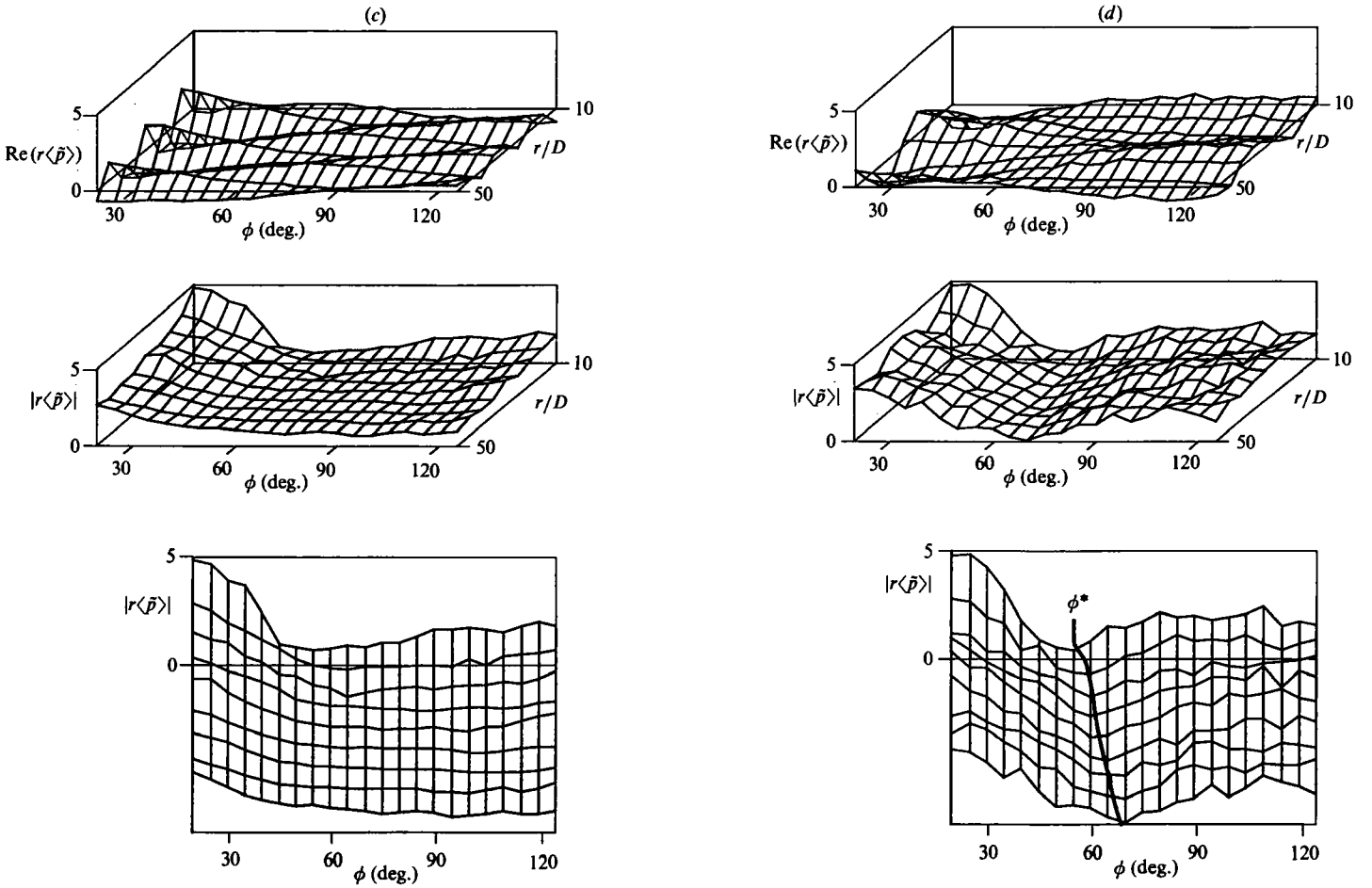

FIGURE 9. Normalized, conditionally averaged sound pressure $\langle \tilde{p}_n \rangle(f)$ in the polar plane ($10 \leqslant r/D \leqslant 50$, $20° \leqslant \phi \leqslant 125°$). Shown are the real part and magnitude (two views) of (*a*) $\langle \tilde{p}_n \rangle(\frac{1}{4}f_{ex})$, (*b*) $\langle \tilde{p}_n \rangle(\frac{1}{2}f_{ex})$, (*c*) $\langle \tilde{p}_n \rangle(\frac{3}{4}f_{ex})$ in SDP flow and (*d*) $\langle \tilde{p}_n \rangle(\frac{1}{2}f_{ex})$ for SP flow. Mesh spacing: $\Delta\phi = 5°$, $\Delta(r/D) = 5$. All sound pressures are scaled by radial distance.

frequency and are not considered here because they are not very compact acoustically. We will focus on the interactions at $x/D \approx 1.0$ ($\frac{1}{2}f_{ex}$) and $x/D \approx 2.0$ ($\frac{1}{4}f_{ex}$) in the SDP flow and the $\frac{1}{2}f_{ex}$ source at $x/D \approx 1.75$ in the SP flow; at these locations the pairing vortices become coplanar.

These data clearly support the simple axisymmetric vortex ring model of the jet used in obtaining the vortex sound theory prediction of the jet sound field.

4.3. *Conditionally averaged measurements of the sound field*

Unfortunately, it is not possible to use the same trigger signal for the sound field because the hot-wire sensor produces its own sound when placed within the flow. This sound cannot be separated from the sound produced by the pairing itself as it is highly correlated with the velocity signal. This is a point studied in detail years ago (Richarz 1980) but often neglected or ignored because of the great temptation to use a hot-wire signal as a trigger for phase-locked measurements of sound. However, the same three conditions which were used in obtaining the conditionally averaged vorticity can be imposed on the sound field to obtain the corresponding conditional average of the sound pressure. For the measurement of the sound, the trigger signal was obtained from a microphone fixed at a point ($r/D = 35$, $\phi = 90°$, $\theta = 90°$) normal to the measurement plane ($10 \leqslant r/D \leqslant 50$, $20° \leqslant \phi \leqslant 125°$, $\theta = 0°$), which itself included the axis of the jet ($\phi = 0°$); see figure 8 for orientation. This arrangement allowed the assumption of axisymmetry to be used as a criterion for the averaging via the cross-correlation between the reference microphone and the measurement microphone (Appendix B). Because of limitations in instrumentation, no condition on the Fourier components was applied to the sound field signals. This was not important for the SDP flow, in which only 0.5% of the measured segments failed to pass such a criterion; however, it undoubtedly caused some smearing of the sound from the SP flow for which some 26% of the periods were discarded by these conditions. For this and other reasons, the SDP flow will receive the most attention in making our comparison with theory. It was also confirmed by detailed tests over several months that the flow was reproducible and therefore was the same during the velocity and sound measurements.

Because the vortex motion and sound are nearly periodic and because the sound source was stationary – i.e. no Doppler shift, an observation found to occur in a wide variety of flows exhibiting pairing (Laufer & Monkewitz 1980; LY; Bridges & Hussain 1987) – the normalized, conditionally averaged sound pressure $\langle p_n \rangle$ will be presented using its first few Fourier coefficients $\langle \tilde{p}_n \rangle(f)$ for $f = \frac{1}{4}f_{ex}, \frac{1}{2}f_{ex}, \frac{3}{4}f_{ex}$ for the SDP flow and $f = \frac{1}{2}f_{ex}$ for the SP flow, avoiding the excitation tone. These (complex) coefficients are plotted in figure 9 as functions of space in the polar plane (r, ϕ). Although the sound is not yet far field, the data are all scaled by the radial distance of the measurement for enhanced clarity. For each spectral component the real part of $\langle \tilde{p}_n \rangle$ is first shown in a wiremesh plot at such an observation angle that the phase of the wave field can be estimated. The magnitude of $\langle \tilde{p}_n \rangle$ is replotted from an angle which shows that the locii of minima in the magnitude field, corresponding to the first angle of extinction ϕ^*, is not a straight radial line. The sound fields show a sharp minimum at polar angles near $\phi = 60°$ with the phase changing sign across this line much as it should if the field were that of an axiquad. Although the measurement region is not truly in the far field of the jet, we see in the data that the extinction angle has begun to reach a constant value with the radius, indicative that the directivity is beginning to reach its far-field limit and that comparison with far-field theory is not invalid.

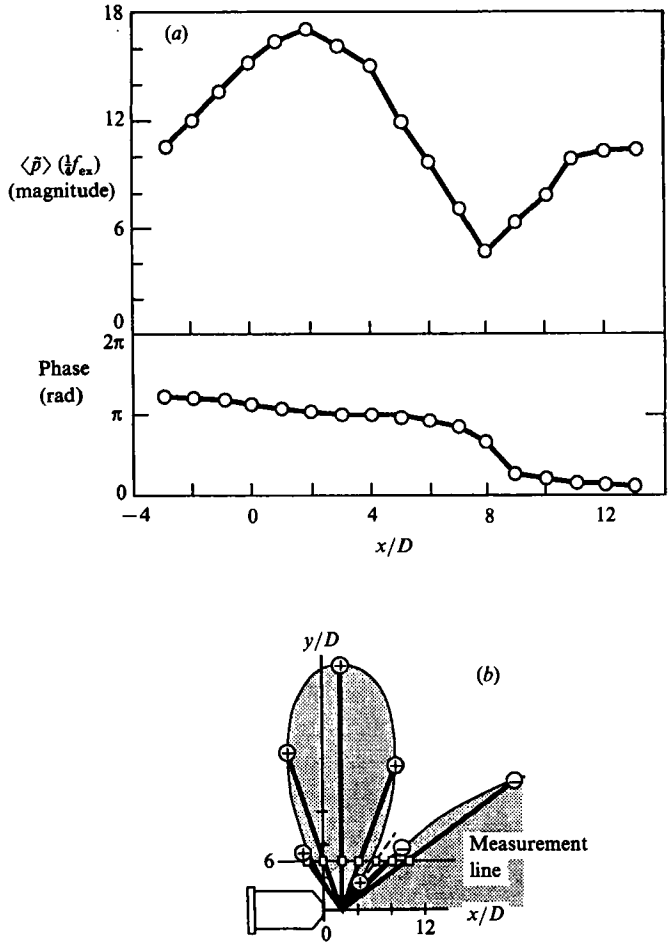

FIGURE 10. Normalized, conditionally averaged sound pressure $|\langle\tilde{p}_n\rangle|(\frac{1}{4}f_{ex})$ in near field ($y/D = 6$) of SDP flow. (*a*) Magnitude (top) and phase (bottom) relative to reference microphone. (*b*) Schematic explaining phase shift observed in (*a*).

4.4. *Near-field verification of single source and source type*

To ascertain that the sound being measured was produced by the vorticity within the field of measurement and not by vortices outside this region, conditionally averaged near-field sound pressure measurements were made just outside the jet along the line $y/D = 6$. Although a measurement based on an acoustic telescope or antennae array might have been made, such techniques cannot be employed if the source is a spatial distribution of multipoles. It is imperative that one assume the form of the source, as a given far field can be produced by a particular spatial distribution of monopoles or dipoles, etc. or by a particular collection of multipoles at a fixed location (as exemplified by Kempton 1976). Since it is the objective of this paper to show that the sound field produced by vortex pairing and predicted by theory is an axiquad, it is pointless to assume this when interpreting the data from a phased microphone array and erroneous to assume that the sources are monopoles as is usually done (e.g. Glegg 1982).

Figure 10 presents the $\frac{1}{4}f_{ex}$ component of the conditionally averaged SDP near-field sound pressure along the axial line $y/D = 6$ in terms of magnitude and phase. The magnitude shows a peak around $x/D = 2$, again coinciding with the location of

pairing. For $x/D > 8$ the magnitude again rises indicating a second source, if one assumes monopole sources. A check of the phase, however, along with the sharpness of the dip at $x/D = 8$, indicates that the rise is merely the second, axial lobe of the axiquad (see figure 10*b*), supporting the inference that the sound field is well represented by an axiquad located near $x/D = 2$. We reiterate that this acoustic source location exercise is only being used as an independent confirmation of the source location, which is determined much more precisely by the conditionally averaged vorticity measurements.

In summary, while it would have been ideal to conditionally average both sound and velocity with the same trigger signal, this could not be done. The method of equivalent conditions outlined above was adequate in this application mostly because of the near-periodicity of the flow which resulted from the very carefully designed, clean flow facility. Although the sound field is not exactly that which was predicted, it is much more like that of the theory than any previous sound measurements in jets, including many excited jet studies (Lush 1971; LY).

5. Discussion

5.1. *Equivalence of educed and simulated vorticity for sound calculations*

Equations (4) and (8) are, in general, difficult to apply to actual flows. To obtain comparable conditional averages of the sound and vorticity, one must use the same criteria for both pressure and vorticity, preferably measuring them both at the same time. Conceptually, this is easy; experimentally, it is very difficult because the insertion of a hot-wire probe into the flow contaminates the jet sound field with the probe-induced flow sound that is highly correlated with the velocity signal. The reciprocal force exerted on the flow by the probe stem as a result of the fluctuations in the velocity is felt as a sound which is highly correlated with the velocity measured by the probe. This sound is not, however, the sound of the flow without the probe and hence this correlation is very biased.

It is also important to note that one cannot use the experimental vorticity data to calculate sound pressure directly. The small, but unavoidable, experimental errors – due primarily to flow reversal and manifested in the temporal fluctuation of conserved integrals of motion such as impulse and moment of impulse – will dominate the result. To reiterate, it is not necessary for the details of the vorticity to be known to compare the directivity predicted by theory and measured in experiments using conditional averages. It suffices to know that the vorticity field is axisymmetric and the approximate location of the vortical motion which creates strong sound pressure changes, e.g. the location where the vortices were coplanar. Details of the vorticity field, such as its distribution in the vortex cores, are important for calculation of the entire sound spectra, i.e. for prediction of the absolute amplitude of different frequency components. Of course, for high harmonics the compact source and flow assumptions will be violated and greater discrepancy between theory and experiment can be expected. As pointed out in the introduction, owing to the linearity of (4), it does not matter if the acoustically compact vorticity field is made up of, say two or two billion axisymmetric vortex rings; the directivity is the same. Therefore, since the theoretical result given by (4) is insensitive to the details of the vorticity field – aside from axisymmetry – the theoretical prediction of the far-field sound pressure at frequency f_c produced by both the SP and SDP vorticity fields is an axiquad under the assumption of axisymmetric compact sources.

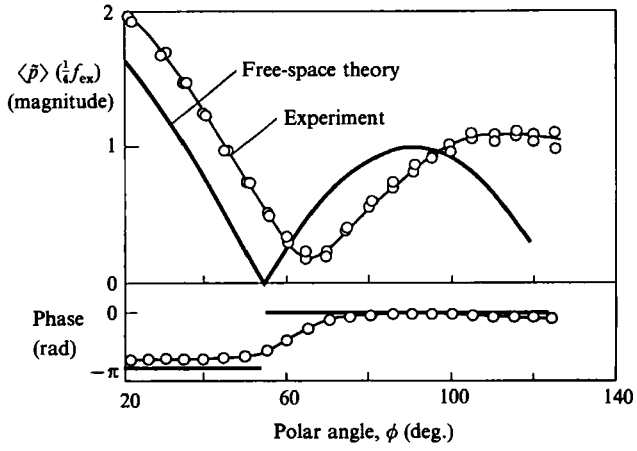

FIGURE 11. Normalized, conditionally averaged sound pressure $|\langle\tilde{p}_n\rangle|(\frac{1}{4}f_{ex})$ at $r/D = 35$ of SDP flow. Experimental data are compared with free-space vortex sound theory applied to vortex pairing.

When comparing the experimental and theoretical results, the $\frac{1}{4}f_{ex}$ data from the SDP flow must be weighed more than the others since the conditions used in averaging vorticity and sound were more nearly the same and for this sound the source is most compact. Figure 11 directly compares the directivity of this sound at $r/D = 35$ to the theoretically predicted axiquad, both in magnitude and phase. There is obviously a sizeable discrepancy between the two which needs to be explained, particularly in the difference in the first extinction angle ϕ^* near 55° and the lack of a second extinction angle ϕ^{**} at 125° in the experimental data. However, most striking to those accustomed to viewing jet noise directivity plots, is the sharp cusp in the conditionally averaged sound field intensity and the relatively distinct phase angle change on either side of this cusp which is a characteristic of the quadrupole. Compared with the monotonic directivity found in most jets, even in those which are excited, the agreement is very close!

5.2. *Possible causes of discrepancy*

To understand whether the discrepancies noted are due to measurement errors, to problems in meeting the assumptions of the theory or to a more fundamental inadequacy of the theory, we will again address the assumptions of the theory and their applicability to our experiments. Then we will consider possible sources of error and evaluate the degree to which the theory can be applied to jet flows.

5.2.1. *Failure to meet conditions of theory*

Inviscid-flow assumption. Although theories exist which account for sound generation by viscous sources, the more simple inviscid theory was used here with the assumption that the flow was essentially inviscid. We can offer no direct proof or calculation beyond that of Obermeier (1985) for dismissing this term. However, we can say that the addition of a viscous monopole would not bring the experimental and theoretical results into better agreement. While adding a monopole of the same sign as the axial lobe of the axiquad would shift the first extinction angle ϕ^* to larger angles, it would also shift the second extinction angle ϕ^{**} to smaller angles where it would be very obvious in the data presented here. We doubt that this assumption accounts for the discrepancy observed.

Compact-source assumption. The axial distance over which vortex motion is

correlated in the jet flows measured here is a few diameters. Our studies covered the range $\lambda/D(= (MSt_D)^{-1}) = [15, 45]$ with $M = 0.08$, where the source region is relatively compact. More importantly, the sound source produced by the periodically pairing vortices was exactly stationary, even though the vortices were advecting at roughly $0.6U$ or $M = 0.05$. Such behaviour can be understood in the light of the fact that, to a far-field observer, the spatially fixed, periodic pairing produces a periodic quadrupole fluctuation at a fixed location, making the source stationary at that frequency and hence as compact as the spatial correlation length l allows. Of course, for frequencies which are not harmonics of the pairing frequency, the evolving vortex pair will appear as an advecting source. Even then, l and D are estimated to be comparable because the vortices produce little sound except for the small time during which they are nearly coplanar (Kambe & Minota 1981).

Surfaces and external sources. The assumption that the flow takes place in a field free from external surfaces was made in the initial stages of the study and at first seemed reasonable. External sources, such as reflections from walls, floors and ceilings, were eliminated by making measurements in an anechoic chamber. Any sound carried down the jet pipe, excluding the intentionally applied excitation tone, was kept, by careful facility construction, to a level where they could not be detected from a point 10 jet diameters away from the nozzle exit. This was confirmed by isolating each potential upstream sound source (blower, chiller, etc.); none produced a detectable difference in the background sound spectra. As the applied excitation consisted of a pure tone with harmonics, only jet noise measured at subharmonics and non-harmonics were considered in his study, their field being uncontaminated by excitation or upstream sources.

Even though the nozzle was designed to present as little reflective surface as possible (Appendix A), it may still have played an important role. The presence of the nozzle body has different effects on the sound field depending upon the wavelength of the sound, the dimensions and geometry of the surface, and the distance between the vortical source region and the surface. In general, the presence of the solid surface can have two effects: first, it can reflect and diffract the free-space axiquad, and second, it can produce a distribution of dipoles on the surface in reaction to the stresses exerted by the flow on the surface. The former effect is expected (based on general results from the theory of scattering waves by solid bodies) to be important when the surface is large compared to an acoustic wavelength, while the latter effect will be strong for low-frequency sound generated by vortical motions very near the nozzle. At high frequencies, for which the nozzle is not acoustically compact, the dipole contributions across the nozzle may constructively or destructively interact, resulting in a complex sound field which is difficult to predict without very detailed information about the dipole distribution and hence the flow–surface interaction (see Goldstein 1976, p. 171).

It is interesting to note two things about the conditional averages of sound pressure which suggest that the dipole term arising from vortex–nozzle interaction is *not* negligible. First, the difference in the first extinction angle ϕ^* between experiment and theory (figure 11) can be removed with the addition of a dipole to the axiquad, the dipole and axiquad being in phase along the positive jet axis. This would also move the second extinction angle ϕ^{**} out of the measurement region, explaining its absence in the data. The second interesting observation is that ϕ^* was not constant with radius (see figure 9). This is not a consequence of the difference between the acoustic source location ($x/D = 2$) and the measurement origin ($x/D = 0$). By simple geometric calculation, this latter effect would cause ϕ^* to be

measured as 45° at $r/D = 10$ and as 52° at $r/D = 50$ rather than the 47° and 65° actually measured. A possible explanation is as follows. The locations where the sound measurements were made correspond to somewhere between near and far field at the wavelengths of concern. In the near field, the dipole and axiquad sound pressure fields have dissimilar dependence on distance: $1/r^2$ for the dipole and $1/r^3$ for the axiquad. If an axial dipole and an axiquad were placed at the same location, ϕ^* would change with radial distance r in the near field, much as it does in the experimental data. It appears that ϕ^* has reached a constant value of 65° by $r/D = 50$, and so it is not likely that this angle will match the theoretical value of 54.7° for an axiquad alone at larger distances. The reader is reminded that the possibility of a dipole source in low-speed jets has been suggested many times previously by researchers observing sound intensities with M^6 scaling, instead of the M^8 scaling of quadrupoles, and by models of the interaction of instability waves with the jet nozzle (Crighton 1972, and references therein). It is possible that the motion of the vortices near the nozzle body is producing a dipole which could improve the agreement between the theory and experiment.

5.2.2. *Error in assuming axisymmetric, periodic vorticity field*

Even though the vorticity field was found to be very nearly axisymmetric, the extreme sensitivity of the theory to small asymmetries in the flow field (Bridges 1990) could have a large effect on the sound. However, by invoking axisymmetry in acquiring the conditional averages of the vorticity and sound fields, any effect on the directivity of the conditional average of the sound has been removed. Experimentally, asymmetry might soften the cusp of the sound field at the extinction angle due to the presence of uncorrelated noise which could not be completely removed in the conditional averaging. This might explain why the SDP flow, which was more axisymmetric and periodic, exhibited a stronger cusp in sound directivity than the SP flow. Deviation from axisymmetry in the experiments of LY might have removed the cusp predicted by HC as well – a possibility not considered in HC.

5.2.3. *Summary of errors made in assumptions*

Of all the assumptions made in this application of vortex sound theory, it appears that the most seriously challenged is the free-space assumption. Work is underway to determine if the surface–vorticity interaction is in fact a sizable source and can account for the majority of the discrepancy found here between the experimental sound field and that predicted by free-space aeroacoustic theory. We suspect that nozzle effects were also the reason that the theory of HC matched so poorly with the data of LY, although it seems likely that the effect is one of reflection instead of an unaccounted-for source from surface/flow interaction due to the small wavelength-to-nozzle-diameter ratio ($= 0.22$) in their experiment.

5.2.4. *Failure of acoustic analogy theory*

The only remaining reason for theory and experiment to disagree is that the theory is inaccurate or incorrect due to the assumption of compact flow. In what way should we suspect the theory to fail? One way is for redirection and re-emission of sound by the vorticity field to dominate the first-order (quadrupole) sound generation terms for some observation angles when the sound must pass through more than one wavelength of vortical flow before reaching the acoustic far field. This effect on the sound directed along the jet is obvious in the zone of silence which it produces. Even in the low-speed jet used here sound intensity is decreased within the jet core (whose

low-frequency hydrodynamic fluctuations make the measurement of sound very difficult at $r/D \leqslant 50$). This signifies that the sound directed along the jet is being redirected to other angles. Some of the differences between the theory and experiment may be explained by the coherent scattering of sound at shallow angles to the jet. Although a detailed analysis is difficult for this situation, it is clear that simple refraction through a thin, steady (time-average) shear layer would redirect sound from small polar angles to larger ones. If this refraction effect is calculated assuming thin shear layers (Goldstein 1976, p. 18), however, the change in both ϕ^* and ϕ^{**} is only a few degrees, not the 10° or more which is observed. It seems more likely that only for angles near the jet axis is the discrepancy due to the refraction effect, which is the failure of the aeroacoustic theory to accurately predict the sound field of the jet. A more exacting study would measure the discrepancy at many different Mach numbers to observe the scaling of the discrepancy with Mach number or frequency. Such a study is impractical, however, because the initial conditions cannot be maintained over a reasonable range of speeds: vortices in the jet become less coherent as the Reynolds number increases, primarily because the boundary layer in the nozzle becomes transitional

6. Summary

Both flow and sound measurements were made in an excited jet in a well-designed, carefully documented facility. The jet was found to be free from facility-dependent artifacts as evidenced by its clean (longitudinal turbulence intensity $u'/U = 0.0004$) velocity field and conventional unexcited jet noise characteristics. When excited at the proper frequencies, axisymmetric vortices were formed which paired periodically at fixed locations; the axisymmetry of the flow field was documented using an azimuthal array of hot wires. The vorticity and sound fields of the jet were measured using conditional averaging to capture the vortex interactions and the sound produced by their motion. The conditions for acceptance of each period of the measured signal were based on amplitude and phase of the signal and on instantaneous axisymmetry. From the conditionally averaged vorticity fields the locations of vortex interaction, and hence of the acoustic source, could be accurately measured.

Inviscid, free-space vortex sound theory was applied to this jet flow under the assumption that the source was acoustically compact (time retardation ignored) and that no solid body was present. This form of the theory was chosen primarily because it is linear in the flow variable, allowing exact comparison of conditionally averaged vorticity and sound pressure, the conditional average being a linear decomposition of the flow variables. The vorticity formulation was also chosen because it is insensitive to most small errors in the vorticity field model; it is only sensitive to deviation from axisymmetry in the vorticity field. The assumption of compact source was supported by the fact that the wavelengths of interest were as much as 45 times the jet diameter, while the free-space assumption was employed mainly for convenience. The theory unambiguously predicts that the far-field sound of axisymmetric vortex pairing in a cold jet at low, but non-zero, Mach number is given by an axisymmetric quadrupole. This theoretical result agreed, to a surprising degree, with the experimental data, which were taken at radial distance only approaching far field.

The primary feature of both theoretical and experimental sound fields is the presence of a polar extinction angle where virtually no sound is heard. The primary

difference between theory and experiment is the exact location of this angle: theoretical value, $\phi = 54.7°$, experimental value, $\phi \approx 65°$. This difference, along with other aspects of the discrepancy between the two fields, hints that the solid body of the nozzle should be considered and the appropriate surface terms included in the theoretical prediction. Depending upon nozzle size, source location and acoustic wavelength, the surface terms would add a dipole source which, when added to the axisymmetric quadrupole, might bring about the requisite change in extinction angle. The discrepancy also supports studies such as Crighton (1972), which argues that neglected nozzle–shear-layer interaction is a strong source of 'excess noise' in jet sound experiments.

At higher frequencies, where the compact-source assumption is less valid, the agreement between theory and experiment worsened as expected. Nevertheless, an extinction angle was found to some degree at all frequencies, again supporting the theoretical prediction that this extinction angle is a fundamental feature of the sound of vortex pairing. Refraction of sound by the jet near the jet axis, which is the expected manifestation of a failure of the theory, seems to limit its applicability to angles away from the jet axis; however, it was not a major factor in the comparison of theory and experiment, made here at polar angles greater than 20°.

Finally, because the sound produced by pairing of axisymmetric vortex rings is given by an axisymmetric lateral quadrupole – very unlike the directivity of practical jet noise – simple axisymmetric vortex pairing cannot be a dominant sound source in cold, low-Mach-number jets as is often claimed. Nor can the directivity usually measured be a result of spatial (axial) and/or temporal jitter in the pairing. At the frequencies bearing most energy, i.e. $St_D \approx 0.3$, the cumulative sound field produced by a spatial distribution of axiquads, even a distribution spanning several jet diameters, would have a directivity which was significantly non-monotonic in polar angle. Either other sound generating mechanisms are stronger than axisymmetric vortex pairing or asymmetry of the vortices is a crucial aspect of the vortex ring interaction. We note that in practical jets there is no potential core; the jet core is itself highly turbulent and thus does not support the formation of axisymmetric vortices. It should not be surprising then to find that axisymmetric vortex pairing is too simple a description for the flow field of practical jets for the purposes of predicting sound generation – a point that we have made many times in the past. It remains to be demonstrated that a simple description of the vortical structures in a jet can be useful in explaining jet noise. If such a description can be found, however, this study indicates that direct application of vortex sound theory will be valid.

This work is one part of the first author's Ph. D. dissertation, which was supported by a NASA Graduate Student Researcher Fellowship and NASA Lewis Research Center Grant NAG-3-639. Additional support for facilities was given ONR Grant N0014-89-J-1361 and Texas State Advanced Research Program grant 202-ARP. The authors are grateful to Mr Arindam Ghosh for his many discussions and thorough review.

Appendix A. Facility and instrumentation

The letters given parenthetically correspond to those in figure 12 which shows the overall design of the experimental facility. A 7-stage blower (A), driven by a 40 h.p. DC motor, is located outside the main building, its outlet connected to the nozzle (L),

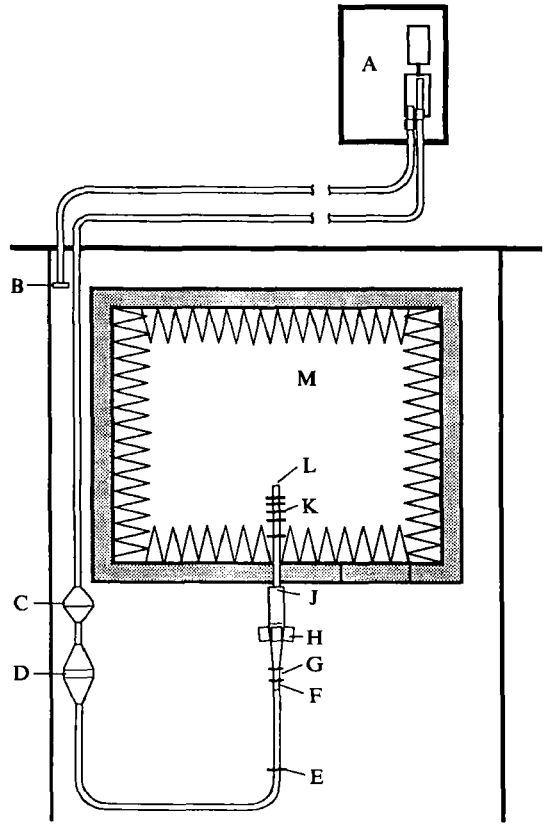

FIGURE 12. Overall view of facility. Letters correspond to description in text.

located in the anechoic chamber (M) via 77 m of 15.25 cm iron pipe. Distances are: (A–C) = 58 m, (C–D) = 2 m, (D–E) = 7.6 m, (E–F) = 2.4 m, (F–L) = 7 m. Between the blower and nozzle are several flow conditioning devices. The air to feed the jet originates from the air-conditioned room (B) which contains the anechoic chamber, allowing the air to be brought back to room condition using a controlled cooling coil (D) for accurate hot-wire measurements; without this, hot-wire signals caused by temperature fluctuations contaminate the velocity signal. Mufflers and vibration isolation couplings located on either side of the blower minimize the sound and vibration which is propagated down the supply pipe and an electrostatic filter (C) removes any dust or dirt which might break hot-wire probes. Large-radius elbows (1 m radius) are used at all bends to minimize secondary flow in elbows which would otherwise produce upstream flow noise and create a strong swirl component in the jet. Although the facility is similar to that used by Hasan & Hussain (1985), for the present work the supply pipe has been extended by 6 m in the laboratory outside the anechoic chamber to allow insertion of the cooling coil (D) and a settling chamber resonance-type excitation device (H) and to allow a longer settling length after the last set of bends. This extension was found to be critical for the flow conditioning, as the flow immediately after the bends is highly asymmetric and has noticeable swirl. At location (E), a specially modified screen was fitted to provide greater pressure drop in those regions of the pipe cross-section where the velocity was higher. This screen removed most of the non-uniformity in the flow profile in the pipe; the swirl component was allowed to persist for over the next 2.4 m straight section to achieve

further cross-stream mixing and symmetrization. At the end of this straight section, a honeycomb (F; cell size: 5×50 mm) removed the remaining swirl before the flow went into the constant-area transition piece (G) and square diffuser. The diffuser had wall angles of 11° and required vanes (2×2) to suppress separation. The inlets of the vanes were sized to account for the momentum deficit at the walls and the outlets were carefully checked to have equal flow, keeping the flow uniform. A coarse screen was added between the vanes and the downstream transition box to remove the wakes of the vanes before the flow was contracted (J) through the anechoic chamber wall. The flow cross-section was again checked after the contraction and was found to be very uniform. A series of screens (K) of decreasing mesh size (24 and 40 mesh) reinitialized the growing boundary layers and reduced the free-stream turbulence intensity to its present low value which is a challenge to measure with conventional instrumentation.

A.1. *Nozzle design*

The axisymmetric contraction nozzle had an inlet diameter of 15.25 cm and an exit diameter $D = 4$ cm, resulting in an area contraction ratio of 14.5. The nozzle was machined from solid aluminium stock and its profile was given by a third-order polynomial with zero-derivative end conditions and a small (1 cm) straight section at the end to allow the streamlines to straighten and avoid separation or formation of a vena contracta. The external geometry of the nozzle is dictated by the shear-layer lip excitation device (not used in this study) designed into the nozzle. The exterior of the nozzle (shown in figure 13) was made into a truncated cone with an included angle of 120° to minimize reflection by the nozzle. This is a clear distinction from the nozzle/excitation design used by LY, where a large (0.9 m) flat plate was fixed to a the exit plane.

A.2. *Temperature control*

To minimize hot-wire velocity measurement error produced by flow temperature variations, a cooling coil was installed in the air supply line. The cooling coil carries chilled water, the temperature control being accomplished by varying the flow rate of the constant-temperature chilled water. The final measured variation in flow temperature for the nozzle configuration and for jet speeds $20 < U_j < 120$ m/s used in this study was ± 0.1 °F over several hours of operation.

A.3. *Excitation system*

Bulk excitation of the jet was provided by making a special chamber to house four speakers angled downstream (figure 13). The speakers excited the longitudinal mode of the cavity resonance of the settling chamber, which induced a purely longitudinal perturbation to the mean flow. This was capable of excitation over a frequency range of roughly $30 < f_{ex} < 1500$ Hz. The 8 in. speakers were placed behind a wall constructed of cotton bedsheet cloth held between two stretched screens (40 mesh). The wall was acoustically transparent, allowing the sound to be efficiently radiated down the tunnel, yet to the flow the wall was hydrodynamically solid and rigid and constituted a smooth continuation of the diffuser. This design allows efficient acoustic input to the chamber without the inherent separation problems which usually attend the insertion of a speaker in the flow or the high losses incurred if the flow is 'seeped' into a settling chamber with a speaker at its end.

All experiments were performed in the University's anechoic chamber. The chamber is a ventilated and air-conditioned concrete box with 0.3 m thick walls set on air bearings with its inner walls covered by fibreglass wedges. The wedges are 1 m

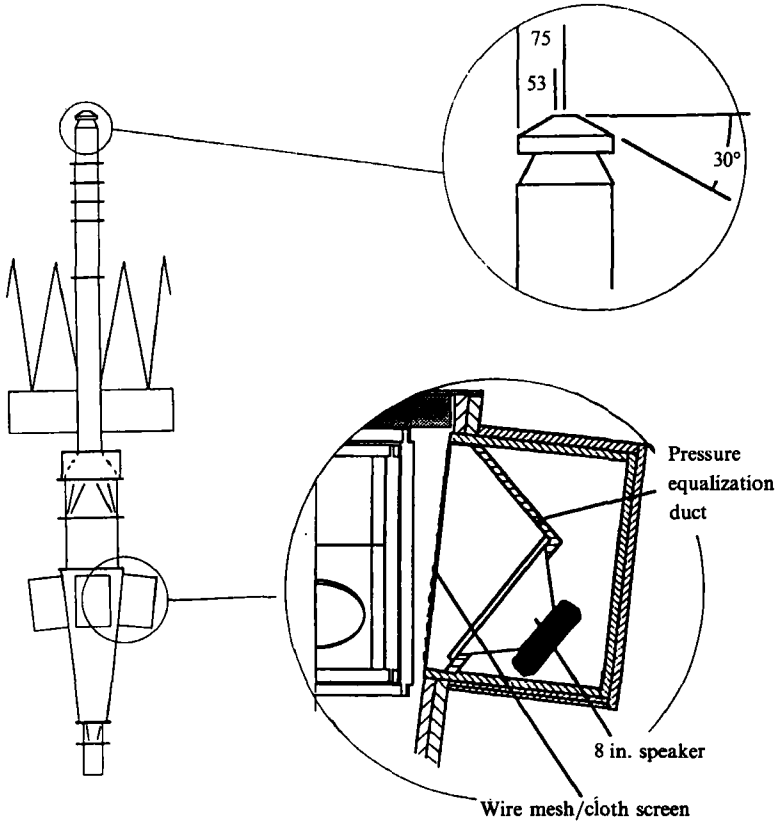

FIGURE 13. Excitation device and nozzle geometry, including inserts showing geometry of speakers and nozzle (dimensions in mm).

long, giving the chamber an ambient sound level of 35 dB above 100 Hz; most of the ambient sound is conducted through the jet pipe from the laboratory outside the chamber. The inside dimensions of the chamber from wedgetip to wedgetip are $7.6 \times 4 \times 5$ m.

A.4. *Facility performance documentation*

Documentation of the flow field and initial condition was hampered in this facility by the difficulty in obtaining a physically steady mount for the traverse in the anechoic chamber. First, the chamber was found to move vertically by about 0.5 mm over a two hour period owing to the unsteady regulation of the air blocks which support the chamber. Second, traverses must be supported on 3 m long pipes which extend up from the floor of the chamber to the level of the wire mesh floor. This allows relative motion between the nozzle and the traverse, which was minimized by tying the traverse to the nozzle; unfortunately, even this introduced perturbation between nozzle and probe due to the vibration of the beams used to tie the traverse and nozzle together. The combined effect is to make the documentation presented here of poorer quality than what we are accustomed to providing. This is not a reflection of the quality of the facility, which is comparable to the best of our other facilities, but is due to constraints of the specialized, anechoic chamber environment.

A traverse set in the vertical plane was used to measure the mean velocity profile across the nozzle (figure 14). The two curves do not precisely align partly because of

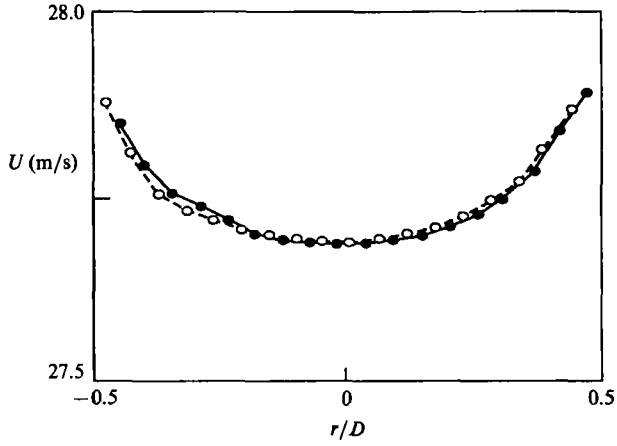

FIGURE 14. Mean longitudinal velocity profiles along vertical and horizontal axes. Open circles are along the vertical axis.

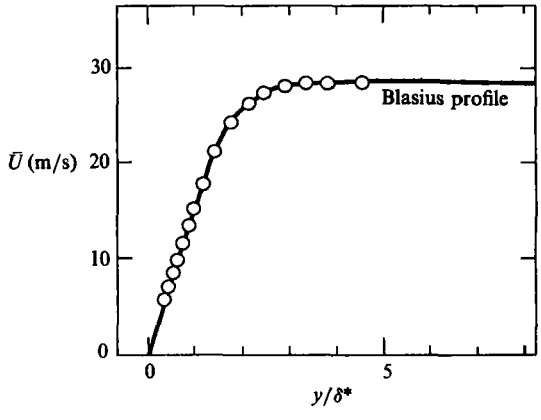

FIGURE 15. Mean longitudinal velocity profile in nozzle boundary layer compared with Blasius profile. δ^* is the displacement thickness.

the relative motion of the nozzle in the vertical direction as the measurement was being made. Interestingly, the very slight overshoot was not found in profiles of total pressure taken with a 0.5 mm Pitot probe; thus it is not due to thermal boundary layers. Figure 15 shows that the mean (longitudinal velocity) boundary-layer profile, having a shape factor of 2.58, is indistinguishable from the Blasius profile.

Movement between nozzle and traverse is especially critical when one is measuring boundary layers with displacement thicknesses less than a millimeter thick, as the vibration of the probe across the boundary layer gives a horrendously high, false value of turbulence intensity. This was ascertained by looking at velocity spectra taken at $y = \delta^*$, where the turbulence intensity is usually found to be maximum even in nominally laminar boundary layers (Hussain 1983). Most of the energy was contained within frequency bands which remain fixed even as the jet speed is varied from 20 to 140 m/s. Experimentation with different vibration reduction methods, which could change the spectral peaks but not completely remove them, determined that this energy was due to vibration of the traverse, traverse support and probe. It was possible to estimate the maximum boundary-layer intensity, arguably the most telling characteristic of the initial condition, by integrating the spectra, neglecting the fixed spectral peaks. Doing this, we obtained figure 16, which shows that the

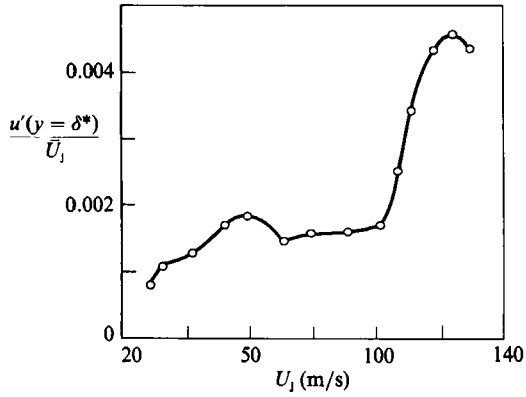

FIGURE 16. Peak longitudinal turbulence intensity in boundary layer as a function of jet speed.

maximum intensity is very low, near that of the free-stream turbulence intensity ($u'/U = 0.0004$ at $U_j = 27.7$), for jet speeds under 100 m/s.

A.5. *Instrumentation*

Most data acquisition and all numerical simulations were performed on Masscomp MC5500 computers. The hot-wire data were acquired with a 12-bit A/D converter through a bank of sample-and-hold amplifier. Sound pressure data were acquired on a two-channel Ono Sokki spectrum analyser because it uses a 16-bit A/D converter which allowed measurement of the low-amplitude sound under the excitation tone (the jet noise was some 30 dB below the imposed acoustic tone).

The hot-wire anemometers were from AA Labs, their signals being converted to velocity digitally using King's law and simple cosine yaw calibration. Three types of probes were employed: a single wire with 5 mm prongs, a single wire with 25 mm prongs, and a crosswire with approximately 5 mm prongs. All used 3.8 μm tungsten-rhodium wire and all had an effective length of approximately 2 mm. The overheat ratio used was 1.5.

Sound measurements were made using two Brüel & Kjaer $\frac{1}{4}$ in. condensor microphones, model 4135, with preamplifier model 2619 and measuring amplifier 2609. The microphones were calibrated using a B&K model 4220 pistonphone.

Two different traverses were used. A horizontal x-y traverse with a spatial resolution of 0.025 mm was used for hot-wire measurements. Microphone measurements were taken using a horizontal angular traverse with a range of polar angles $\pm 125°$, the microphone being moved by hand along the boom over a range of $10 \leqslant r/D \leqslant 50$. Larger radii were not possible with this range of polar angles, and the sound intensity was to low to measure accurately at much larger radii, anyway. The measured angular accuracy was 0.25° with repeatability of 0.5°. The reference microphone used in eduction was located vertically above the jet exit at $r/D = 35$, giving data from a direction normal to the plane of the angular traverse. The microphone was mounted on a stinger 1.1 m above the boom, which was 25 mm wide and covered in cotton batting to minimize reflection.

Appendix B. Conditional average via a far-field transfer function

In the following, standard signal processing notation, such as is used in Bendat & Piersal (1980), is employed to analyse and justify the use of the transfer function between orthogonal points in the sound field as a conditional average of the

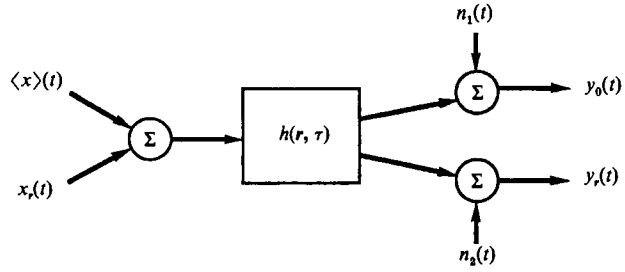

FIGURE 17. Model used in signal processing.

axisymmetric sound pressure. Initially, the problem is stated as a signal processing problem with multiple input and output, shown schematically in figure 17. The inputs, $\langle x\rangle(t)$ and $x'(t)$, are the linearly independent components (conditional average and remainder, respectively) of the vorticity field. These vortical motions can be considered via vortex sound theory to be the physical sources of sound. The linear and causal transfer function $h(\boldsymbol{r},\tau)$ given by vortex sound theory maps near-field vorticity to far-field pressure at location $\boldsymbol{r}$. The output $y_0(t)$ and $y_r(t)$ are the sound measured at a reference point and at the point $\boldsymbol{r}$, respectively. The additive noise terms $n_1(t)$ and $n_2(t)$ would be sound from non-vortical sources, such as the excitation system.

The conditionally averaged vorticity was measured under the constraints that periods of the field were axisymmetric and met threshold criteria on the Fourier series coefficients at $\frac{1}{4}f_{\mathrm{ex}}$ and $\frac{1}{2}f_{\mathrm{ex}}$. If the latter criteria are dropped and the reference point is chosen appropriately, the conditional average procedure can be implemented using standard transfer functions since the temporal conditions revert to the simple time average. Because the Fourier series coefficient criteria dismissed only 0.7% of the periods of the SDP flow, dropping these criteria did not noticeably change the quantity educed. This also allows one to apply a common result for multiple, uncorrelated inputs:

$$G_{\langle x\rangle y}(f) = H(f)[G_{\langle x\rangle\langle x\rangle}(f)+G_{\langle x\rangle x'}(f)].$$

Allowing that $G_{\langle x\rangle x'}(f)$, the cross-correlation of conditional average and remainder, is zero by definition, one obtains

$$H(f) = \frac{G_{\langle x\rangle y}(f)}{G_{\langle x\rangle\langle x\rangle}(f)}.$$

Furthermore, it was found that at the frequencies of interest, specifically *not* at harmonics of the excitation frequency, the output noise n_1 and n_2 either were not correlated or were small.

Now, one may consider the cross-spectrum between two microphones and separate the transfer function $H(f)$, which is a function of microphone position, into two functions, one for each microphone. $H_0(f)$ will be the transfer function for the reference microphone while $H_r(f)$ will the transfer function for a microphone at field location $\boldsymbol{r}$. This is given by

$$G_{y_0y_r}(f) = H_0^*(f)\,H_r(f)\,G_{\langle x\rangle\langle x\rangle}(f).$$

Because $G_{\langle x\rangle\langle x\rangle}(f)$ is a scalar, the equation can be divided by it, giving

$$H_0^*(f)H_r(f) = \frac{G_{y_0y_r}(f)}{G_{\langle x\rangle\langle x\rangle}(f)}.$$

From the definition of a transfer function,

$$G_{y_0 y_0} = |H_0|^2 G_{\langle x\rangle\langle x\rangle},$$

the above expression becomes

$$H_0^* H_r = \frac{G_{y_0 y_r}|H_0|^2}{G_{y_0 y_0}}.$$

Then,

$$H_0 H_0^* H_r = \frac{G_{y_0 y_r}|H_0|^2 H_0}{G_{y_0 y_0}} = |H_0|^2 H_r,$$

$$H_r = \frac{G_{y_0 y_r} H_0}{G_{y_0 y_0}}.$$

If the transfer function H_0 is used as a reference (choosing a reference point where H_0 is non-zero), then the normalized directivity is simply

$$\frac{H_r}{H_0} = \frac{G_{y_0 y_r}}{G_{y_0 y_0}}.$$

This is the normalized conditionally averaged sound pressure field, which is easily interpreted at 90° as being the fraction of the sound field at the given frequency which is axisymmetric.

REFERENCES

Ahuja, K. K. 1973 *J. Sound. Vib.* **29**, 155.

Bendat, J. S. & Piersal, A. G. 1980 *Engineering Applications of Correlation and Spectral Analysis*. Wiley.

Bridges, J. E. 1990 Application of coherent structure and vortex sound theories to jet noise: Ph.D. Thesis, University of Houston.

Bridges, J. E. & Hussain, A. K. M. F. 1987 *J. Sound Vib.* **117**, 289.

Broadbent, E. G. & Moore, D. W. 1979 *Phil. Trans. R. Soc. Lond.* A**290**, 353.

Crighton, D. G. 1972 *J. Fluid Mech.* **56**, 683.

Crighton, D. G. & Huerre, P. 1990 *J. Fluid Mech.* **220**, 355.

Crow, S. C. 1970 *Stud. App. Maths* **46**, 21.

Curle, N. 1955 *Proc. R. Soc. Lond.* A**231**, 505.

Ffowcs Williams, J. E. & Hall, L. H. 1970 *J. Fluid Mech.* **40**, 657.

Glegg, S. A. L. 1982 *J. Sound Vib.* **80**, 31.

Goldstein, M. E. 1976 *Aeroacoustics*. McGraw-Hill.

Hasan, M. A. Z. & Hussain, A. K. M. F. 1985 *J. Fluid Mech.* **150**, 159.

Howe, M. S. 1975 *J. Fluid Mech.* **71**, 625.

Huerre, P. & Crighton, D. G. 1983 *AIAA 8th Aeroacoustics Cong. AAIA*-83-0661 (referred to herein as HC).

Hussain, A. K. M. F. 1983 *Phys. Fluids* **26**, 2816.

Kambe, T. 1984 *J. Sound Vib.* **95**, 351.

Kambe, T. 1986 *J. Fluid Mech.* **173**, 643.

Kambe, T. & Minota, T. 1981 *J. Sound Vib.* **74**, 61.

Kempton, A. J. 1976 *J. Sound Vib.* **48**, 475.

Laufer, J. & Monkewitz, P. 1980 *AIAA 6th Aeroacoustics Conf. AAIA*-83-0661.

Laufer, J. & Yen, T.-C. 1983 *J. Fluid Mech.* **134**, 1 (referred to herein as LY).

Lighthill, M. J. 1952 *Proc. R. Soc. Lond.* A**211**, 564.

LUSH, P. A. 1971 *J. Fluid Mech.* **46**, 477.
MÖHRING, W. 1978 *J. Fluid Mech.* **85**, 685.
MÖHRING, W. 1990 *J. Sound Vib.* **140**, 155.
MOORE, C. J. 1977 *J. Fluid Mech.* **80**, 321.
OBERMEIER, F. 1985 *J. Sound Vib.* **99**, 111.
POWELL, A. 1964 *J. Acoust. Soc. Am.* **36**, 177.
RICHARZ, W. G. 1980 *J. Acoust. Soc. Am.* **67**, 73.
ZAMAN, K. B. M. Q. & HUSSAIN, A. K. M. F. 1978 *J. Fluid Mech.* **87**, 349.
ZAMAN, K. B. M. Q. & HUSSAIN, A. K. M. F. 1980 *J. Fluid Mech.* **101**, 449.